GRAPHENE OXIDE-LOADED SHORTENING AS AN ENVIRONMENTALLY-FRIENDLY HEAT TRANSFER FLUID WITH HIGH THERMAL CONDUCTIVITY

Thammasit VONGSETSKUL*[1], Peeranut PRAKULPAWONG[1], Panmanas SIRISOMBOON[2], Jonggol TANTIRUNGROTECHAI[1], Chanasuk SURASIT[1], Pramuan TANGBORIBOONRAT[1]

[1]Department of Chemistry, Faculty of Science, Mahidol University, Rama VI Road, Ratchathewi, Bangkok 10400, Thailand

[2]Department of Mechanical Engineering, Faculty of Engineering, King Mongkut's Institute of Technology Ladkrabang, Bangkok 10520, Thailand

*Corresponding author e-mail: thammasit.von@mahidol.ac.th, Tel: +66 2201-5933, Fax: +66 2354-7151

Abstract

Graphene oxide-loaded shortening (GOS), an environmentally-friendly heat transfer fluid with high thermal conductivity, was successfully prepared by mixing graphene oxide (GO) with a shortening. Scanning electron microscopy revealed that GO particles, prepared by the modified Hummer's method, dispersed well in the shortening. In addition, the latent heat of GOS decreased while their viscosity and thermal conductivity increased with increasing the amount of loaded GO. The thermal conductivity of the GOS with 4% GO was higher than that of pure shortening of ca. 3 times (from 0.1751 to 0.6022 [$Wm^{-1}K^{-1}$]) and increased with increasing temperature. The GOS started to be degraded at ca. 360 °C. After being heated and cooled at 100 °C for 100 cycles, its viscosity slightly decreased and no chemical degradation was observed. Therefore, the prepared GOS is potentially used as environmentally friendly heat transfer fluid at high temperature.

Key words: *graphene oxide; heat transfer fluid; shortening; thermal conductivity*

1. Introduction

Heat transfer fluid (HTF) is a liquid substance used to carry heat away from its source to be cooled. It is used to monitor heat and temperature [1] and determine the efficiency of heat utilization in various applications such as chemical processing, concentrated solar power, food and beverage processing, pharmaceutical and plastic processing and system maintenance. In solar thermal energy, the solar collectors convert solar radiation into heat that transfers through HTF to a heat exchanger [2]. This heat boils water and produces steam. Since the electricity is obtained from turbine driven by steam, it is directly proportional to the amount of heat transferred to water.

Based on the operation temperatures, HTF can be classified as low and high temperature ones. Water-based liquid containing alcohol or diol is low temperature HTF whereas petroleum-based and synthetic mineral oils such as silicone and paraffinic oil, alkylated aromatic and fluorocarbon are used

at high operating temperature. However, these high temperature HTFs are not biodegradable and not derived from renewable resources. Thus, shortening, a mixture of fatty acid and triglycerides of vegetable origin, is introduced for environmental-friendly reason. Although it is non-toxic, normally used at high temperature, non-corrosive and cost-effective, its thermal conductivity (TC), necessary to prevent failures during instantaneous overload, is low. To enhance the TC of HTFs, highly thermal conductive materials such as active carbon in lauric acid [3], carbon fibers in paraffin [4], carbon nanotubes in palmitic acid [5], exfoliated graphite in wax/LDPE [6], expanded carbon in capric-myristic acids [7], expanded graphite in palmitic acid [8] and nanographite in paraffin waxes [9] have been added to improve TC of HTF.

Among various nanomaterials with high surface area [10-18], graphene is probably the most suitable carbon-based nanomaterial to increase TC of HTF due to its low thermal interface resistance associated with their two-dimensional planar structure [19]. The viscosity of graphene-based suspension decreased at relatively high loading, whereas a monotonic increase was observed for suspensions with all the other carbon additives. Unfortunately, a single layered graphene is hard to be produced in large amount; therefore, graphene oxide (GO), produced on the ton scale in inexpensive ways [20-21], is potentially to be used to improve TC of materials instead.

Due to the relative ease of GO production, in this contribution, GO was added into shortening to generate naturally derived and biodegradable HTFs with high TC used at high temperature for the first time. The thermal properties, thermal stability, morphology and viscosity of the developed GO-loaded shortening (GOS) were investigated by thermogravimetric analyzer (TGA) and differential scanning calorimeter (DSC), Fourier transform infrared spectroscopy (FTIR), scanning electron microscope (SEM) and rotational viscometer, respectively.

2. Experimental

2.1 Materials

Graphite (< 20 μm, Sigma-Aldrich, USA), hydrogen peroxide (H_2O_2, 30%, Univar, Australia), potassium permanganate ($KMnO_4$, Univar, Australia), shortening (Crisco, USA), sodium nitrate ($NaNO_3$, Univar, Australia) and sulfuric acid (H_2SO_4, 98%, RCI Labscan, Thailand) were used as received. The deionized (DI) water was used throughout this work.

2.2 Preparation of GO and GOS

GO particles were prepared by the modified Hummer's method [22]. In brief, graphite powder (5 g), $NaNO_3$ (2.5 g) and 98% H_2SO_4 (115 ml) were mixed together and stirred at 0 °C for 10 min. After the slow addition of $KMnO_4$ (15 g), the mixture was warmed up to 35 °C while stirred for 30 min. DI water (250 ml) was gradually added. The mixture was heated at 98 °C for 15 min and cooled in a water bath for 10 min. Subsequently, DI water (700 ml) and 30% H_2O_2 (5 ml) were slowly added. After being stirred at room temperature for 30 min and left standing for a day, the dark green precipitate was collected and washed, by decantation and centrifugation at 3,300 rpm for 30 min, with DI water 4 times. The obtained GO powders were dried on a freeze dryer (Supermodulyo-230,

Thermo Scientific, USA) before mixing with melted shortening (60 °C) at mass fractions of 1, 2, 3 or 4% w/w. The prepared GOS were then cooled down to room temperature.

2.3 Characterization of GO particles and the GOS

The morphologies of graphite, GO powders and GOS were observed under SEM (TM-1000, Hitachi, Japan). Their XRD patterns were recorded on X-ray diffractometer (XRD, D8 ADVANCE, Bruker, USA) operating at 40 kV and 40 mA using high power $CuK_{\alpha 1}$ radiation with Ge-crystal (Johansson type) monochromator (λ = 1.5406 Å). The diffraction patterns were examined at 5 – 80° with a scanning rate of 1 s/step and a step size of 0.075°. TC of the GOS (30 ml) was measured at 30, 60 and 90 °C using the transient hot-wire method [23-26], i.e., the thermostat with a sensor (Thermal Logic, USA) with a diameter of 1.27 mm, a length of 60 mm, a voltage of 1.6 V and a power of 1.8 W was immersed into the samples. Each set of the experiment was conducted in triplicate. The average values and their errors were reported.

The latent heat of the samples was determined by DSC (DSC1, Mettler Toledo, The Netherlands) from 0 to 100 °C at the heating and cooling rates of 10 °C/min under nitrogen atmosphere. TGA (TGA-7, Perkin Elmer, USA) was performed on a thermal analyzer varying from 50 to 550 °C at a heating rate of 10 °C/min under nitrogen atmosphere. The chemical compositions of shortening, GO powders and the GOS were characterized by FTIR (Equinox 55, Bruker, Germany). Its chemical degradation was also observed by FTIR. The viscosity of the melted GOS was measured by a rotational viscometer (VT-04F, Rion, Japan) with a rotor speed of 62.5 rpm and the aid of an adaptor for liquids with low viscosities at 60 °C. To assess thermal stability, the GOS with 4% w/w GO was heated up to 100 °C and cooled down to 30 °C for 100 cycles. The viscosity of the GOS was measured for every 10 cycles at 60 °C. It should be noted that each set of the viscosity measurements was conducted in triplicate. The average values and their errors were also reported.

3. Results and discussion

XRD patterns of graphite and synthesized GO powders are shown in fig.1

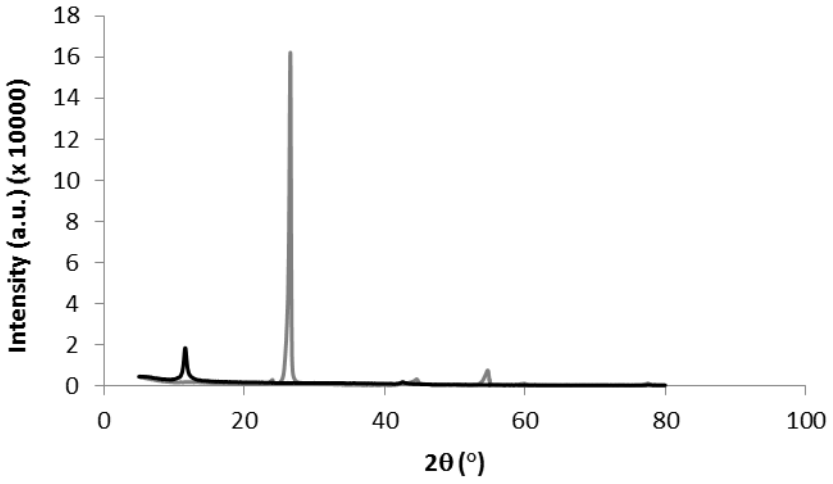

Figure 1 X-ray diffraction spectra of graphite powder (gray) and graphene oxide (black)

The peaks at 26.6, 41.9 and 54.1° in the XRD spectrum (a) correspond to the layered structure of graphite [27]. In contrast, the spectrum (b) shows only a broad characteristic peak at 11.5°, matching with that of GO [28]. The absence of high intensity sharp peaks indicates that the layers of graphene in graphite were exfoliated. In addition, the existence of only a peak in spectrum (b) confirms the significant purity of the synthesized and purified GO powders possibly resulted from several oxygenated groups on the GO sheets [29-30]. The morphologies of graphite, synthesized GO and the GOS with 4% w/w GO were studied under SEM and their images are shown in fig. 2a), 2b) and 2c), respectively.

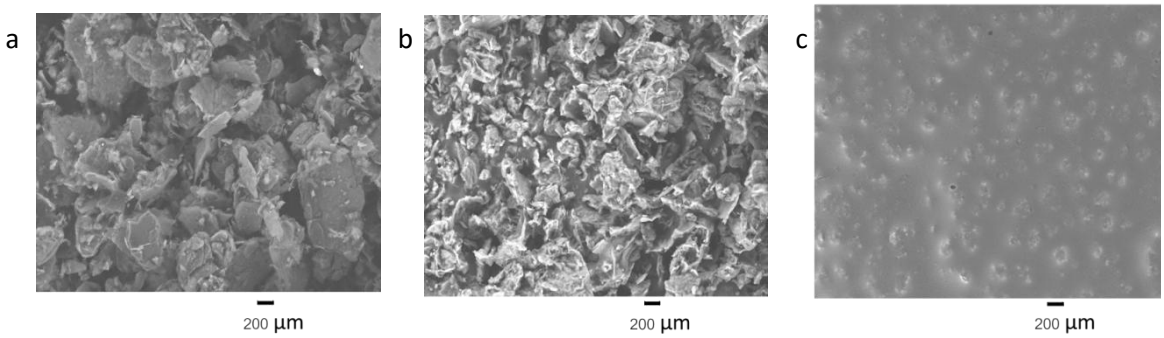

Figure 2 Scanning electron micrographs of a) graphite, b) graphene oxide and c) graphene oxide-loaded shortening with 4% w/w graphene oxide

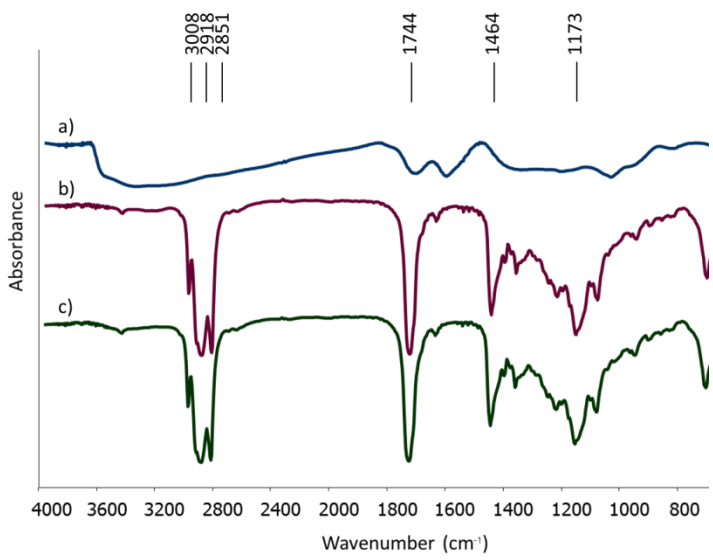

Figure 3 Fourier transform infrared spectroscopy spectra of a) graphene oxide, b) shortening and c) graphene oxide-loaded shortening with 4% w/w graphene oxide

SEM micrographs revealed that the size of graphite particles in fig. 2a) was larger and its surface was smoother when compared to GO in fig. 2b). This indicated that the stacks of graphene in graphite were disintegrated resulting in the increase in surface area of the resulting GO particles. fig. 2c) reviewed that GO with an average size of 123±33 µm well dispersed in the shortening probably due to

the presence of oxygen-containing functional groups on the GO surface preventing the agglomeration. This would benefit the increase in TC of the GOS which involves the collision of the particles in the materials via the convection mechanism [24]. If the particles agglomerated, the number of the particles collisions and TC of the materials would also decreased. To investigate the functional groups existed in GO and the interaction with shortening, FTIR was used for analysis of GO, shortening and the GOS. Their spectra are displayed in fig. 3.

The spectrum a) of GO in fig. 3 shows the three broad bands, i.e., ~1850 – 3600 (carboxylic groups), ~1700 (C=O carboxylic acid stretching) and ~1600 cm^{-1} (aromatic groups) whereas the characteristic peaks at 2851, 2918, 3008 (-CH_3 stretching) and 1744 cm^{-1} (C=O stretching of ester groups) appear in the spectra b) and c) of shortening and GOS [31]. The identical IR spectra b) and c) and no peak shift in the GOS spectrum could be implied that the shortening and GO were physically mixed without chemical interaction between two phases. Next, the relation between TC of the GOS and the amount of added GO at 30, 60 and 90 °C is shown in fig. 4a), 4b) and 4c), respectively.

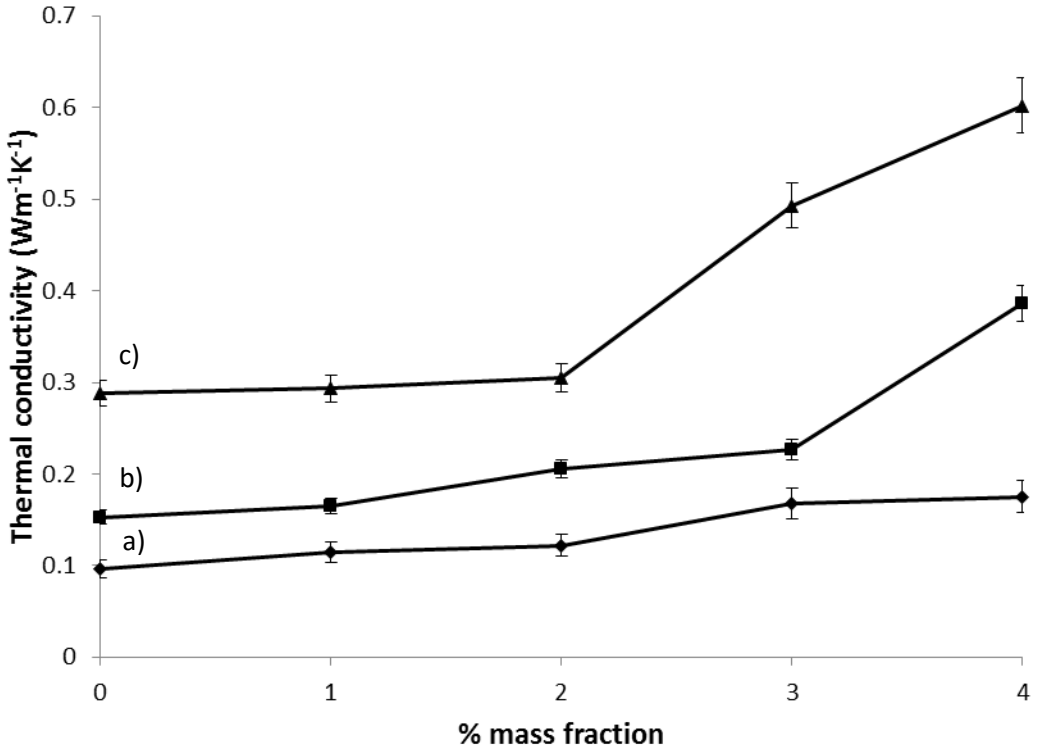

Figure 4 Thermal conductivity of graphene oxide-loaded shortening *vs.* % graphene oxide mass fraction at a) 30, b) 60 and c) 90 °C)

Results in fig. 4 suggest that the TC of all the GOSs increased with increasing the temperature and the amount of added GO. It was explained that the increase in temperature caused an increase in the number of particle collisions and, as a result, TC of the GOS [24]. However, at 30 °C, the addition of GO hardly affected the TC of GOSs (fig 4a) whereas the TC of the GOSs at 60 and 90 °C greatly

increased with increasing the GO content from 3 to 4% and from 2 to 4%, respectively (fig. 4b and 4c). The minimum amount of the added GO particles to start the heat transfer via a collision mechanism decreased with increasing temperature. This probably resulted from the ease of GO particles collision. Moreover, the shortening melted at ca. 47 – 48 °C which facilitated the movement of the added GO particles. When the numerical values of TC were considered, it was found that TC of the GOS with 4% GO was ~2.5 and ~2 times higher than that of pure shortening at 60 and 90 °C, respectively.

It was found that the ability of GO to enhance TC of shortening was not much different from the other organic materials. For example, in 2013, TC of palmitic acid increased about three to four times after being added by GO [32]. In 2014, reduced GO, a derivative of GO, was added to polystyrene. The results showed that TC of polystyrene was enhanced by almost twice as the reduced GO concentration increased from 0 to 10% vol. [33].

Not only TC but also the viscosity of the GOS is important because it controls the ability of HTFs to be flowed in pipes, which is vital in practical uses. Then, the relation between the viscosity of the GOS and the amount of GO added into the GOS at 60 °C was studied. The graph is shown in fig. 5.

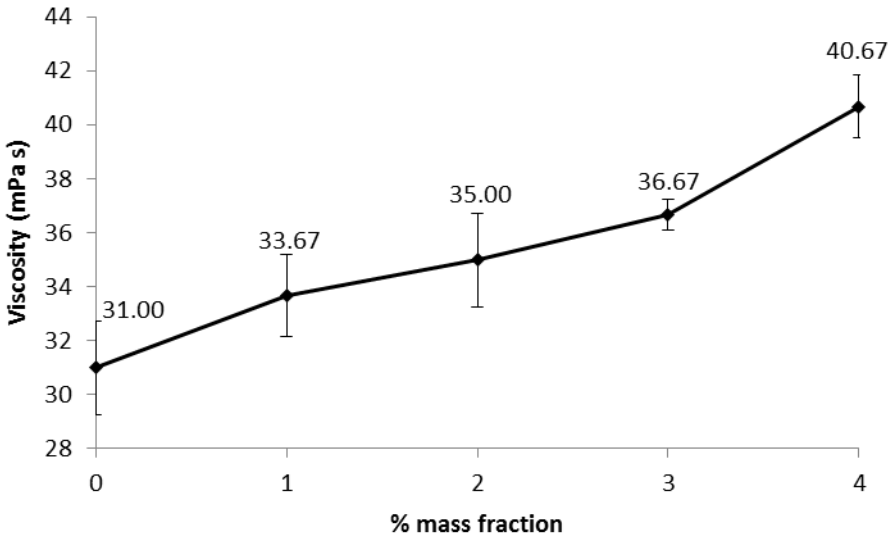

Figure 5 The viscosity of graphene oxide-loaded shortening as a function of % graphene oxide mass fraction

It was observed that the viscosity of the GOS composites linearly increased with increasing the GO mass fraction or the volume fraction of the suspended particles [34]. Even though the TC of GOS with 4% w/w GO was higher than that of pure shortening more than twice, the viscosity of GOS (41 mPa·s) was ca. 1.3 times of that of pure shortening (31 mPa·s). This yielded the highly thermal conductive HTFs which could be flowed easily.

The latent heat, the thermal energy released or absorbed by a material and one of the important indexes for being good HTFs, of the GOS was then determined. The DSC thermograms of pure shortening and the GOS with various amounts of loaded GO powders are shown in fig. 6.

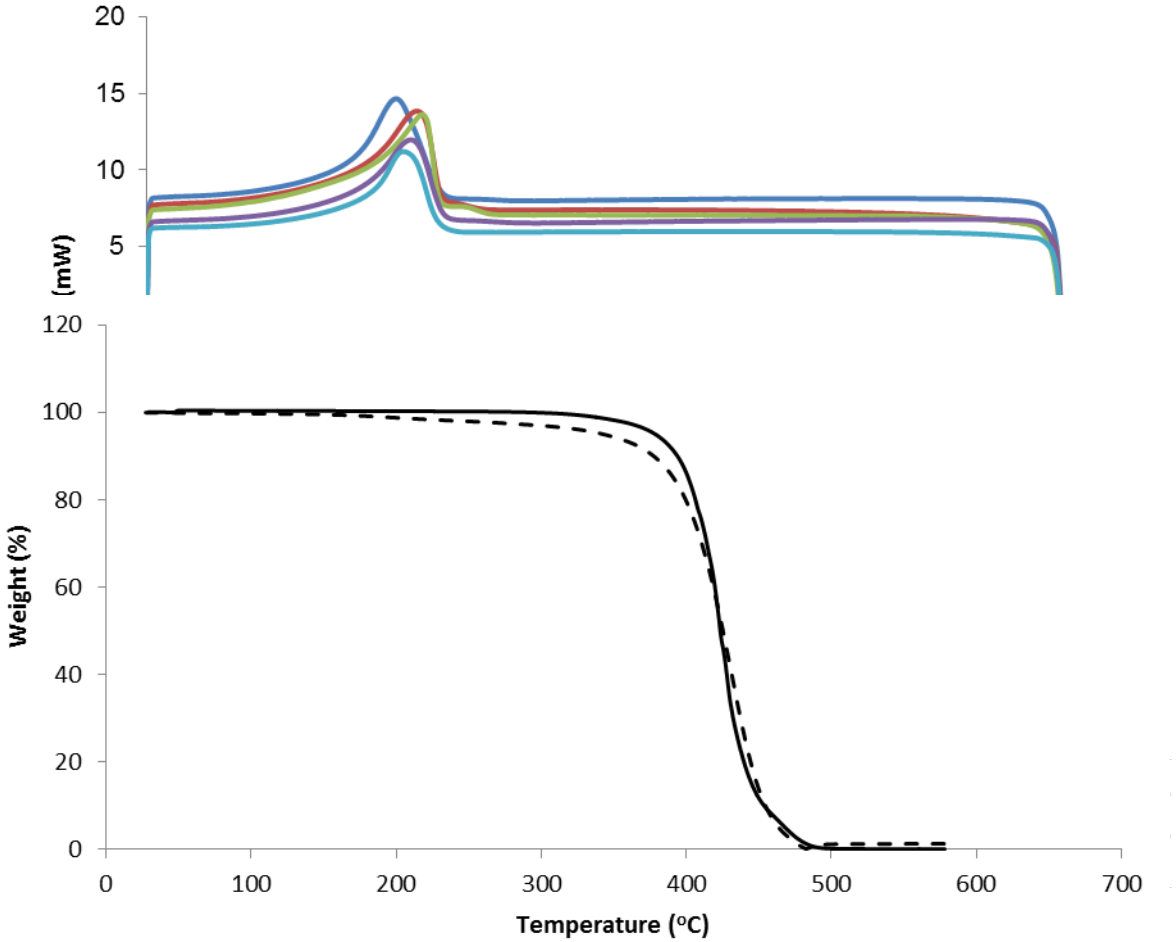

In fig. 6, the shapes and the phase change temperatures of all DSC thermograms were almost similar. The melting and the freezing temperatures of all the GOSs were ca. 46 and 29 °C, respectively. This confirmed no chemical interaction between shortening and GO and no relation between the amount of added GO and the melting temperature of the GOS. To understand the change in the enthalpy of melting and freezing and the relation between the enthalpies and the amount of added GO, the latent heats of the GOSs are calculated and the data are shown in tab. 1.

Table 1 The relation between % graphene oxide mass fraction in graphene oxide-loaded shortening and the enthalpy of melting and freezing & the phase change temperature of the GOS

% Graphene oxide	$\Delta H_{melting}$ (J/g)	$\Delta H_{freezing}$ (J/g)	Melting temperature (°C)	Freezing temperature (°C)
0	20.2	15.7	27.6	45.8
1	19.9	14.4	29.7	46.0
2	19.2	13.8	39.2	46.4
3	18.8	12.9	28.9	45.8
4	18.7	12.8	28.1	46.2

Tab. 1 reveals that the reduction in the enthalpy of melting and freezing the GOS is proportionally to the amount of loaded GO. However, there are only small differences between the enthalpies of melting and freezing of the GOS with 3% w/w GO and those with 4% w/w GO, indicating the onset of the phase separation between shortening and GO at 4% w/w GO. To balance the homogeneity and the enhancement of the TC, the GOS with 4% w/w was chosen for the study of the thermal stability.

In addition, adding GO into shortening did not affect both melting and freezing temperatures. These results were consistent with FTIR results (fig. 3) that the shortening and GO were physically mixed only. Thermal decompositions of shortening and GOS with 4% w/w GO mass fraction were determined by TGA. The thermograms are shown in fig. 7.

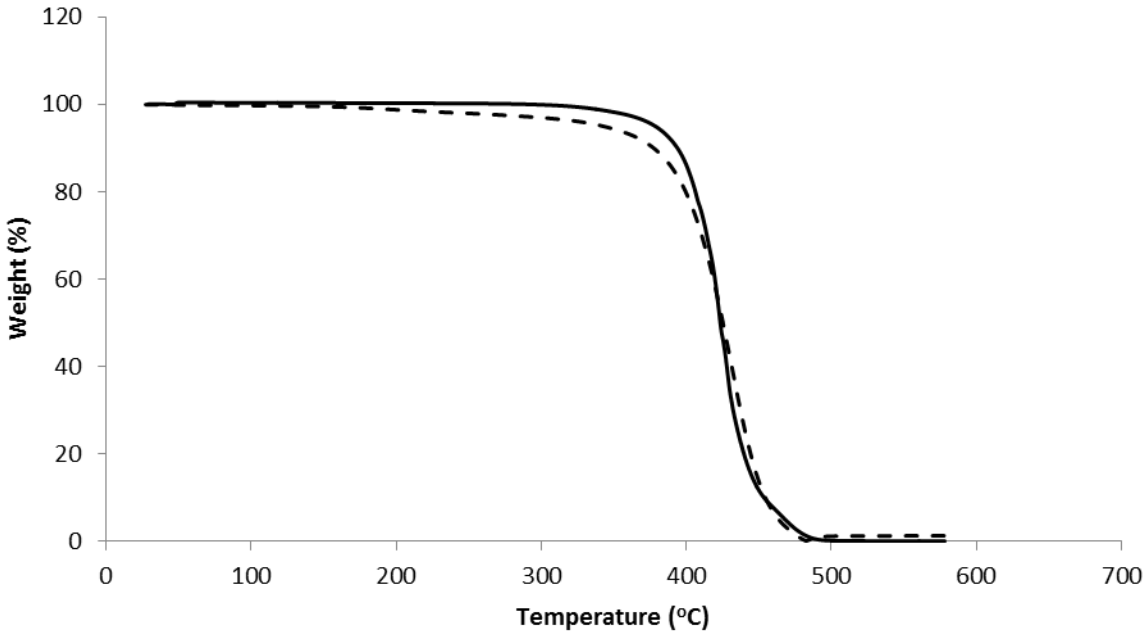

Figure 7 Thermogravimetric thermograms of shortening (solid line) and graphene oxide-loaded shortening with 4% w/w graphene oxide (dash line)

The TGA thermograms show that initial decomposition temperature of the shortening and the GOS composites were ca. 360 °C. The slight change in the degradation of the shortening indicates the good thermal stability of the GOS and confirmed no chemical interaction between shortening and GO as formerly observed from the DSC studies [35]. To further investigate the thermal stability of the GOS with 4% w/w GO, the chemical degradation of the GOS before and after being heated and cooled for 100 cycles was examined by FTIR. It was found that the FTIR spectrum of both the freshly prepared and used GOS were identical which supports no chemical degradation and oxidation of the GOS after being heated and cooled for 100 cycles. Therefore, the GOS with 4% w/w GO could be used as HTFs for at least 100 cycles. The viscosity of HTFs was also measured and the results are shown in fig. 8.

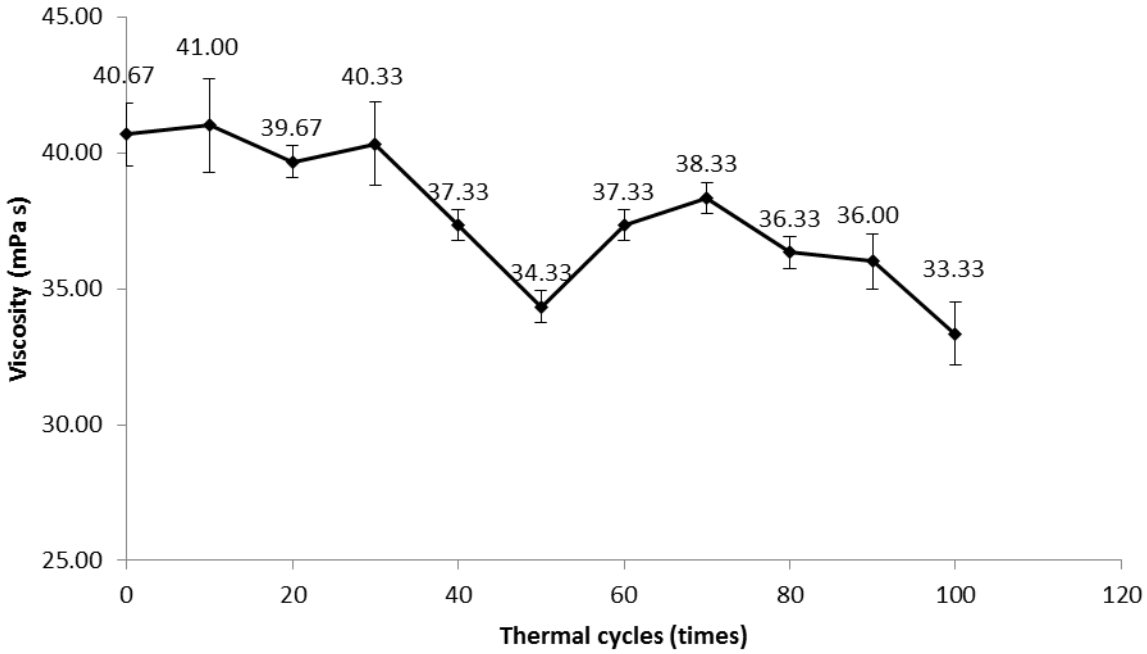

Figure 8 The relation between the viscosity of graphene oxide-loaded shortening with 4% w/w graphene oxide and the number of thermal cycles

The viscosity of the GOS with 4% GO slightly decreased after being heated and cooled for 100 cycles because some of the long hydrocarbon chains of the heated shortening were probably cut. Thus, all the results indicate the great potential of the GOS with 4% w/w GO to be used as HTFs at high temperature.

4. Conclusion

The GOS, an environmentally-friendly HTF with high thermal conductivity (0.6022 [$Wm^{-1}K^{-1}$]) for being used at high temperature, was successfully prepared by mixing 4% w/w GO with a shortening. SEM images showed that GO particles dispersed well in shortening. DSC thermograms revealed that the latent heat of the GOS slightly decreased while their viscosity and TC increased from 31.00 to 40.67 mPa·s and from 0.1751 to 0.6022 [$Wm^{-1}K^{-1}$], respectively, with increasing the amount of loaded GO and temperature from 0 to 4% w/w and from 30 to 90 °C, respectively. TGA thermograms indicated that the GOS started to be degraded at ca. 360 °C. Results from FTIR and viscometer can be implied that, after being heated and cooled at 100 °C for 100 cycles, its viscosity slightly decreased from 40.7 to 33.3 mPa·s without chemical degradation. Thus, the GOS with 4% w/w GO would be potentially used as HTF at high temperature.

Acknowledgements

Research grants from The Thailand Research Fund (TRF)/Mahidol University (TRG5680070), Mahidol University Faculty of Science and Thailand Ministry of Science and Technology to T.V. and from TRF/Commission on Higher Education to P.T. (RTA5480007) are gratefully acknowledged. The

authors also express sincere thanks to Mettler Toledo (Thailand) for providing DSC facility to carry out in this research work.

References

[1] Harris, A., *et al.*, Measuring the thermal conductivity of heat transfer fluids via the modified transient plane source (MTPS), *J. Therm. Anal. Calorim.*, *116* (2014), 3, pp. 1309-1314

[2] Liu, J., *et al.*, Thermodynamic properties and thermal stability of ionic liquid-based nanofluids containing graphene as advanced heat transfer fluids for medium-to-high-temperature applications, *Renew. Energ.*, *63* (2014), pp. 519-523

[3] Chen, Z., *et al.*, Synthesis and thermal properties of shape-stabilized lauric acid/activated carbon composites as phase change materials for thermal energy storage, *Sol. Energ. Mat. Sol. C.*, *102* (2012), pp. 131-136

[4] Elgafy, A., Lafdi, K., Effect of carbon nanofiber additives on thermal behavior of phase change materials, *Carbon*, *43* (2005), pp. 3067–3074

[5] Wang, J., *et al.*, Increasing the thermal conductivity of palmitic acid by the addition of carbon nanotubes, *Carbon*, *48* (2010), pp. 3979-3986

[6] Wang, J., *et al.*, Enhancing thermal conductivity of palmitic acid based phase change materials with carbon nanotubes as fillers, *Sol. Energ.*, *84* (2010), pp. 339–344

[7] Karaipekli, A., Sari, A., Capric–myristic acid/expanded perlite composite as form-stable phase change material for latent heat thermal energy storage, *Renew. Energ.*, *33* (2008), 12, pp. 2599-2605

[8] Sari, A., Karaipekli, A., Preparation, thermal properties and thermal reliability of palmitic acid/expanded graphite composite as form-stable PCM for thermal energy storage, *Sol. Energ. Mat. Sol. C.*, *93* (2009), pp. 571-576

[9] Li, M., A nano-graphite/paraffin phase change material with high thermal conductivity, *Appl. Energ.*, *106* (2013), pp. 25-30

[10] Moghadam, A., *et al.*, Effects of CuO/water nanofluid on the efficiency of a flat-plate solar collector, *Exp. Therm. Fluid Sci.*, *58* (2014), pp. 9-14

[11] Ho, C., *et al.*, Thermal performance of Al_2O_3/water nanofluid in a natural circulation loop with a mini-channel heat sink and heat source, *Energ. Convers. Manage.*, *87* (2014), pp. 848-858

[12] Khaleduzzaman, S., *et al.*, Energy and exergy analysis of alumina–water nanofluid for an electronic liquid cooling system, *Int. Commun. Heat Mass*, *57* (2014), pp. 118-127

[13] Ho, C., Lin, Y., Turbulent forced convection effectiveness of alumina–water nanofluid in a circular tube with elevated inlet fluid temperatures: an experimental study, *Int. Commun. Heat Mass*, *57* (2014), pp. 247-253

[14] Karami, N., Rahimi, M., Heat transfer enhancement in a PV cell using Boehmite nanofluid, *Energ. Convers. Manage.*, *86* (2014), pp. 275-285

[15] Akhavan-Behabadi, M., *et al.*, An empirical study on heat transfer and pressure drop properties of heat transfer oil-copper oxide nanofluid in microfin tubes, *Int. Commun. Heat Mass*, *57* (2014), pp. 150-156

[16] Rimbault, B., *et al.*, Experimental investigation of CuO–water nanofluid flow and heat transfer inside a microchannel heat sink, *Int. J. Therm. Sci.*, *84* (2014), pp. 275-292

[17] Maddah, H., *et al.*, Experimental study of Al_2O_3/water nanofluid turbulent heat transfer enhancement in the horizontal double pipes fitted with modified twisted tapes, *Int. J. Heat Mass Tran., 78* (2014), pp. 1042-1054
[18] Naik, M., *et al.*, Comparative study on thermal performance of twisted tape and wire coil inserts in turbulent flow using CuO/water nanofluid, *Exp. Therm. Fluid Sci., 57* (2014), pp. 65-76
[19] Yu, Z., *et al.*, Increased thermal conductivity of liquid paraffin-based suspensions in the presence of carbon nano-additives of various sizes and shapes, *Carbon, 53* (2013), pp. 277-285
[20] Mehrali, M., *et al.*, Shape-stabilized phase change materials with high thermal conductivity based on paraffin/graphene oxide composite, *Energ. Convers. Manage., 67* (2013), pp. 275-282
[21] Park, S., Ruoff, R., Chemical methods for the production of graphenes, *Nat. Nanotechnol., 4* (2009), pp. 217-224
[22] Marcano, D., *et al.*, Improved synthesis of graphene oxide, *ACS Nano, 4* (2010), 8, pp. 4806-4814
[23] Håkansson, B., Ross, R., Effective thermal conductivity of binary dispersed composites over wide ranges of volume fraction, temperature, and pressure, *J. Appl. Phys., 68* (1990), 2533, pp. 3285
[24] Moroe, S., *et al.*, Thermal conductivity measurement of gases by the transient short-hot-wire method, *Exp. Heat Transfer, 24* (2011), pp. 168-178
[25] Healy, J., *et al.*, The theory of the transient hot-wire method for measuring thermal conductivity, *Physica B & C, 82* (1976), 2, pp. 392-408
[26] Alvarado, S., *et al.*, A hot-wire method based thermal conductivity measurement apparatus for teaching purposes, *Eur. J. Phys., 33* (2012), 4, pp. 897-906
[27] Sun, G., *et al.*, Preparation and characterization of graphite nanosheets from detonation technique, *Mater. Lett., 62* (2008), pp. 703-706
[28] Dmitriy, A., *et al.*, Preparation and characterization of graphene oxide paper, *Nature, 448* (2007), pp. 457-460
[29] Park, S., *et al.*, Colloidal suspensions of highly reduced graphene oxide in a wide variety of organic solvents, *Nano Lett., 9* (2009), 4, pp. 1593-1597
[30] Nair, R., *et al.*, Unimpeded permeation of water through helium-leak–tight graphene-based membranes, *Science, 335* (2012), 6067, pp. 442-444
[31] McMurry, J., *Organic Chemistry*, Brooks/Cole, China, 2012
[32] Mehrali, M., *et al.*, Preparation and properties of highly conductive palmitic acid/graphene oxide composites as thermal energy storage materials, *Energy, 58* (2013), pp. 628-634
[33] Park, W., *et al.*, Electrical and thermal conductivities of reduced graphene oxide/polystyrene composites, *Appl. Phys. Lett., 104* (2014), pp. 113101
[34] Thomas, D., Transport characteristics of suspension: VIII. a note on the viscosity of Newtonian suspensions of uniform spherical particles, *J. Colloid Sci., 20* (1965), 3, pp. 267-277
[35] Fahlman, B., *Materials Chemistry*, Springer, Netherlands, 2011